STUDY ON THE FATIGUE FAILURE OF A COBALT HARDFACED STEEL SHAFT

A.A. FERNANDES, V.T.A. ANTUNES, P.M.S.T. DE CASTRO*

The present study describes a failure examination conducted on a shaft of an oil-extracting press. The causes of the failure were traced to manufacturing faults and service loading conditions. Crack growth under Mode III conditions occurs. An attempt was made to use fracture mechanics principles to predict the fatigue behaviour of the shaft. Limitations in using these techniques are apparent due to lack of data on Mode III crack growth and K_{III} solutions.

INTRODUCTION

Shafts of rotating equipment are often subjected to complex histories of high torques. This situation can lead to crack growth under Mode III conditions. The present study describes a failure examination conducted on a shaft of an oil-extracting press. The shaft with a helicoid is used to transport and compress the seeds from which the oil is extracted.

The aim of the present paper is to report the causes which lead to the service failure. The shaft broke in two parts which were used for metallographic and fractographic examinations.

Since the shaft is subjected in service to cyclic torques, an attempt was made to estimate the fatigue life of the shaft using a fracture mechanics approach.

SERVICE CONDITIONS

The shaft is subjected to compression and torque loads and transmits 36.8 kW at 45 rpm. The hollow shaft is water-cooled, the maximum temperature on the surface being estimated at less than 100°C. The heating effect is due to severe abrasion wear induced by the compressed seeds.

*Oporto University, Faculty of Engineering, Rua dos Bragas 4099 OPORTO, Portugal.

Several superficial cracks could be observed on planes perpendicular to the axis. The location of the final fracture is shown in Figure 1.

MATERIALS

The original shaft is made of a low alloy steel with the chemical composition shown in Table 1.

TABLE 1 - Shaft Base Material

	C	Mn	P	S	Si	Cu	Cr	Ni	Mo	Sn	Al
%	.42	.96	.01	.033	.32	.22	1.03	.16	.23	.01	.039

The material was used in the annealed condition, with a hardness of 199 HV5. The shaft is originally hard-faced with a 27% Cr - 15% Fe cobalt-based alloy, with 2 mm thickness, giving a surface hardness of 494 HV5.

A detailed failure examination was conducted on samples taken from the fracture surface as shown in Figure 2.

Main cracks were found to be located at points of high stress concentration near the root of the helicoid. Cracks propagate through the wear-resistant overlay into the base material and extensive crack branching was found. The fracture surfaces presented tightly adherent compressed seeds, as shown in Figure 3.

The examination was conducted on samples taken from the body of the shaft and the root of the helicoid.

FAILURE MECHANISMS

Metallographic Examination

Optical metallography was carried out in a section of the body of the shaft as sketched in Figure 4. The sample revealed a 1.5 mm-thick wear-resistant overlay. This overlay was deposited using a spray technique which gives a very low dilution with the base material as can be seen in Figure 5. The hard facing operation produced a heat-affected zone displaying two distinct zones marked B and C on Figure 5. Zone B, with a width of approximately 0.1 mm, corresponds to austenitized material. The microstructure is essentially formed by ferrite and fine perlite. Zone C, approximately 7 mm wide, has not reached austenitizing temperature and presented a tempered microstructure. Hardness tests in these two zones gave the following values:

Zone B - 286 HV5
Zone C - 303 HV5 (max.)

Sections through the root of the heicoid are presented in Figure 6. The analysis of these macrographs revealed interesting points, namely:

- the helicoid is not machined, but built up by welding.
- the original shaft was reclaimed in successive operations, as revealed by the identification of several different alloys. The chemical composition of these alloys is shown in Table 2.

TABLE 2 - Chemical Composition of Built-up Alloys

%	Si	Mn	Cr	Ni	Fe
R1	1.8	0.4	7.8	-	bal
R2	1.5	<0.3	6.0	-	bal
R3	1.4	-	10.6	2.2	bal
R4	1.4	-	17	8.7	bal

The welding operation used to build the helicoid produced a heat-affected zone, with hardness above 400 HV, clearly shown in Figure 6. The extensive cracking observed in the heat-affected zone leads to the conclusion that an inadequate welding procedure was used. They appear to be hydrogen-induced cold cracks. A probable cause of their occurrence would be, among others, lack of preheat during the welding operation.

The hard facing of the shaft presented several surface cracks of a variable size and orientation. The successive hard overlay deposits with various chemical compositions originated internal cracks in some points (solidification and/or reheat cracking).

Microfractography

The observation of the fracture surfaces using a Scanning Electron Microscope revealed a smooth flat fracture without any morphologic features which could help to identify the failure mechanism, as seen in Figure 7. The fracture surface shows signs of severe rubbing which is fractographically identical to pure cyclic Mode III surfaces reported by Ritchie (1) for an identical steel. The shaft base material has a low toughness, as concluded by final fracture surface appearance, illustrated in Figure 8, where cleavage facets are clearly visible, indicating a brittle-type fracture.

FATIGUE LIFE PREDICTIONS

A stress analysis of the shaft under service conditions was carried out. The coefficient of friction seeds/inner surface of the cylinder containing the shaft was estimated as 0.3, (2). The pressure on the seeds is estimated as 0.44 Nmm^{-2} minimum, and the shaft is subjected to an axial compressive load of 102.9 KN. Maximum nominal shear stress, on a plane perpendicular to the axis is $\tau = 17\ Nmm^{-2}$, whereas on this plane a nominal compressive normal stress of $\sigma_c = 25\ Nmm^{-2}$ is found. This analysis reveals a substantial safety factor for the shaft.

A fracture mechanics approach was used to carry out a fatigue life assessment of this shaft. The use of fracture mechanics to estimate fatigue life under Mode I loading conditions is widely known and applied. Mode III applications are

far less well documented, both as far as K_{IIIc} and crack growth data are concerned; crack growth in Mode III can be characterised by the relationship

$$\frac{da}{dN} = f(\Delta K_{III})$$

Both types of data for a steel similar to the shaft base material could however be found in the literature. K_{IIIc} data was found in (3), whereas crack growth rate data was recently presented by Ritchie et al. (1).

The stress intensity factor solution for the circumferentially-notched cylindrical bar subjected to a given torque T is given by Rooke and Cartwright in ref. (4):

$$K_{III} = \frac{2\,R_2\,T}{(R_2^4 - R_1^4)}\sqrt{\frac{a}{\pi}}\quad Y = K_o\,Y$$

where a is crack depth, R_2 is outside radius and R_1 is inside radius. The data thus assembled was used to carry out a fatigue life estimate. Some assumptions were made. A straight line corresponding to the upper boundary of da/dN versus ΔK_{III} data (1) was adopted for the present study. Initial cracking occurred near the root of the helicoid. To take into account the root stress concentration effect, the nominal tangential stress for crack depths up to 13 mm were multiplied by estimated stress concentration factors. R was assumed to be 0, i.e. $\Delta K_{III} = K_{III\ max}$.

Using the K_{IIIc} data from (3), it was observed that conditions for unstable crack growth due to

$$K_{III} = K_{IIIc}$$

were not found even for very large values of crack depth.

The fatigue crack growth study is summarised in Table 3. Initial crack depth a_i was estimated as 3 mm. Final crack depth was estimated as 46 mm, and nine intervals were used to compute the number of cycles. For each interval the crack growth rate was taken as the value corresponding to the higher limit.

TABLE 3 - Crack Growth Data

a	K_o	K_{III}/K_o	SCF	K_{III}	da/dN
mm	$MNm^{-3/2}$	= Y		$MNm^{-3/2}$	mm/cycle
8	2.694	1.0	2	5.34	2×10^{-7}
13	3.435	1.1	1.5	5.67	2.2×10^{-7}
18	4.042	1.25	1	5.05	1.4×10^{-7}
23	4.569	1.5	1	6.85	3×10^{-7}
28	5.041	1.9	1	9.58	1×10^{-6}
33	5.473	2.5	1	13.68	3.6×10^{-6}
38	5.873	3.6	1	21.14	1.5×10^{-5}
43	6.247	6.2	1	38.73	1×10^{-4}
46	6.461	8.1	1	52.33	3×10^{-4}

This study gives an estimated life for the component of 10.7×10^7 cycles. The computations shown above assume a regular growth of the crack, i.e., a circumferential notch of increasing depth. Examination of the final fracture revealed that the growth was irregular, the fatigue crack being deeper in certain radial directions, and shallower in others. In some directions, it reached the inner surface of the shaft. Final crack length assumed in the calculations in Table 3 should not be taken as a rigorous estimate. For fatigue life calculations, however, errors in the evaluation of crack length for final catastrophic fracture are of little importance, due to the high values of the growth rates, as is well known.

DISCUSSION

Metallographic and microfractographic analyses indicate that inadequate manufacturing and repair procedures were adopted, as proven by the extensive internal and external cracking present in the shaft. These cracks were the initiation points of main cracks which propagated throughout the shaft until final fracture. The presence of the external helicoid in the shaft introduced an additional stress concentration which, coupled with the presence of cracks, created the conditions for their propagation. No definitive conclusions as far as the adequacy of shaft base material could be drawn since no mechanical tests were carried out. Figure 8 suggests that the base material had a low toughness.

The shaft was subjected, in service, to torsion loading. This type of loading, Mode III, is known to produce rubbing and oxidation of the fracture surfaces in the process of crack propagation, which makes it difficult to characterize the fracture mechanism involved only by fractographic analysis.

An attempt was made to use a fracture mechanics methodology to analyse the fatigue behaviour of the shaft. The purpose was twofold: to study the significance of the initial surface cracks, and to study the influence of the quality of base material under the present loading conditions. The shaft is hard-faced, as already mentioned; if the hardness of the overlay is very high, in excess of 600 HB as is the case, it is difficult to deposit the weld metal and avoid the occurrence of small cracks which, for static loading, have no deleterious effect. In a dynamic situation, however, they can have a detrimental effect on the fatigue behaviour, as the present study reveals. The fracture mechanics calculations carried out to predict the fatigue behaviour under Mode III cyclic loading, revealed to be feasible but difficulties still subsist, namely the availability of appropriate ΔK_{III} solutions and crack growth data.

The results of this study, rather than trying to present a fundamental analysis of the problem, serve to illustrate the present limitations and the need for more data to become available.

CONCLUSIONS

- Inadequate manufacturing and repair procedures were considered to be the main causes of the failure of the shaft.

- Fracture surfaces produced by cyclic Mode III loading cannot be characterized by fractographic analysis due to the rubbing and oxidation which occur.

- Crack growth data under Mode III loading and K_{III} solutions were found to be scarce, although they are essential to the proper analysis of failures of many machine elements.

SYMBOLS

a	- crack depth
K_{III}	- Mode III stress intensity factor
K_{IIIc}	- Mode III fracture toughness
R	- cyclic load ratio (min/max)
R_1	- inside radius
R_2	- outside radius
T	- twisting moment
τ	- shear stress
σ	- normal stress

REFERENCES

1. Ritchie,R.O., McClintock,F., Nayeb-Hashemi,H., Ritter, M.A., "Mode III fatigue crack propagation in low alloy steel", (Metallurgical Transactions A, Vol 13A, January, 1982) 101-110.

2. Reimbert,M., Reimbert,A., "Silos: Théorie et Pratique", (Eyrolles, 1971).

3. Hurd,N.J., Irving,P.E., in: Proceedings of the Third European Congress on Fracture, (ECF3, J.C. Radon ed., Pergamon Press, 1980) 239.

4. Rooke, D.P., Cartwright, D.J., "Compendium of Stress Intensity Factors", (Her Majesty's Stationery Office, 1976), 239.

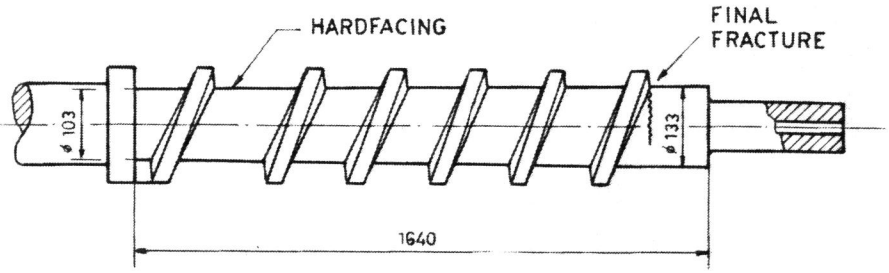

FIG. 1 - Shaft showing location of final fracture

FIG. 2 - Final fracture surface

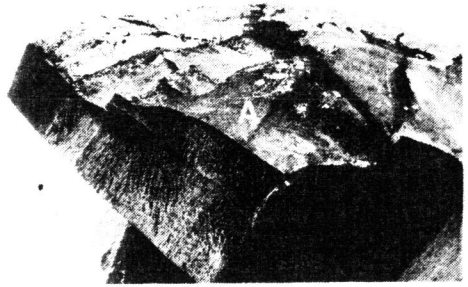

FIG. 3 - Crack branching

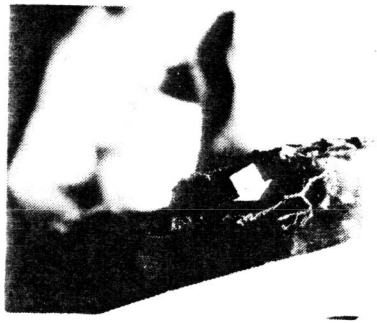

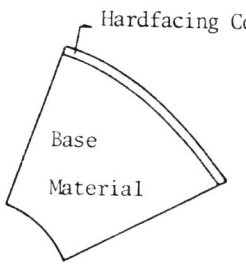

FIG. 4 - Surface cracks within the shaft body starting at the wear resistant overlay (left).
Cross section of shaft body (right).

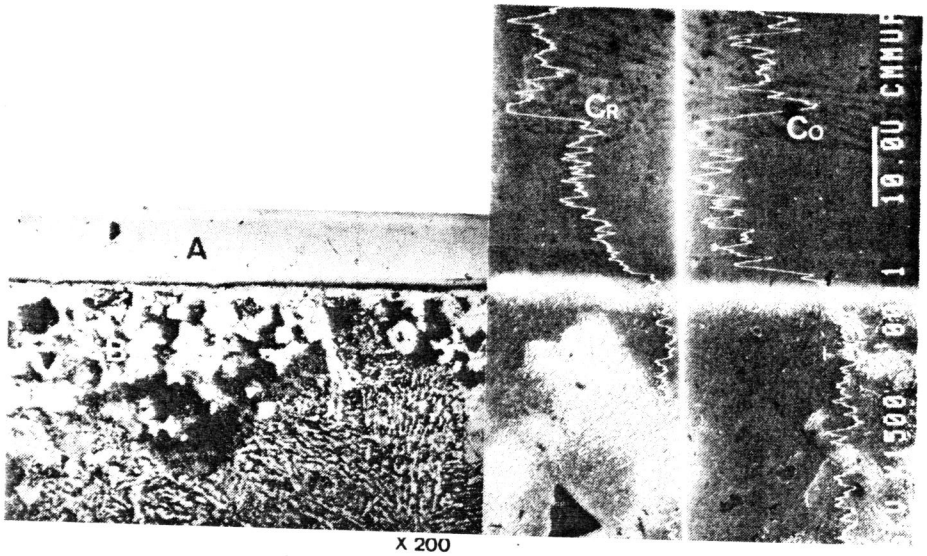

FIG. 5 - Heat affected zone produced by spray hardfacing (left):
A - Co alloy
B - Austenitized base material
C - Non - Austenitized base material
Interface Cobalt alloy - base material with two line scannings for Cr and Co (right).

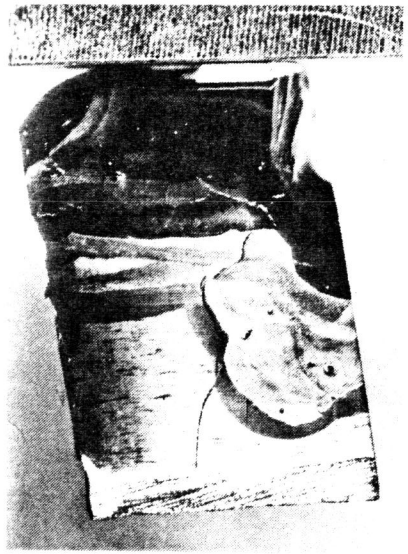

FIG. 6 - Heat affected zone cracking produced during helicoid build up

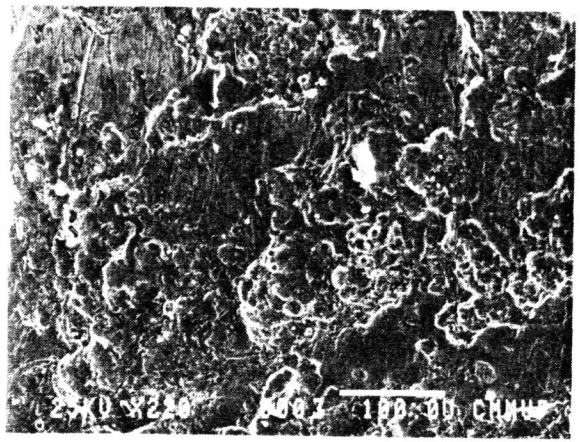

FIG. 7 - Microfractography of fracture surface

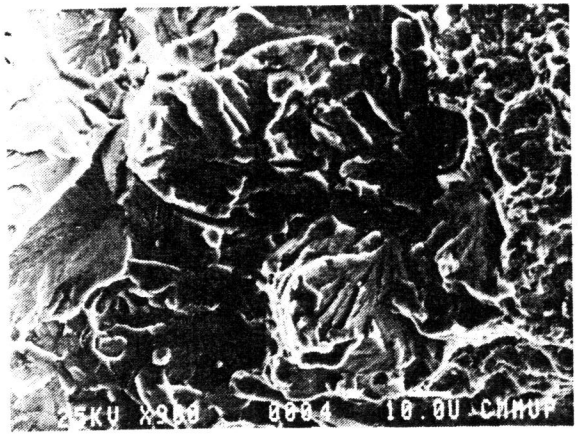

FIG. 8 - Brittle type fracture showing cleavage facets.